Organic electrochemical transistors

Jonathan Rivnay[1], Sahika Inal[2], Alberto Salleo[3], Róisín M. Owens[4], Magnus Berggren[5,6] and George G. Malliaras[7]

Abstract | Organic electrochemical transistors (OECTs) make effective use of ion injection from an electrolyte to modulate the bulk conductivity of an organic semiconductor channel. The coupling between ionic and electronic charges within the entire volume of the channel endows OECTs with high transconductance compared with that of field-effect transistors, but also limits their response time. The synthetic tunability, facile deposition and biocompatibility of organic materials make OECTs particularly suitable for applications in biological interfacing, printed logic circuitry and neuromorphic devices. In this Review, we discuss the physics and the mechanism of operation of OECTs, focusing on their identifying characteristics. We highlight organic materials that are currently being used in OECTs and survey the history of OECT technology. In addition, form factors, fabrication technologies and applications such as bioelectronics, circuits and memory devices are examined. Finally, we take a critical look at the future of OECT research and development.

[1]*Department of Biomedical Engineering, Northwestern University, Evanston, IL, USA.*
[2]*Biological and Environmental Sciences and Engineering Division, King Abdullah University of Science and Technology (KAUST), Thuwal, Kingdom of Saudi Arabia.*
[3]*Materials Science and Engineering, Stanford University, Stanford, CA, USA.*
[4]*Department of Chemical Engineering and Biotechnology, University of Cambridge, Cambridge, UK.*
[5]*Laboratory of Organic Electronics, ITN, Linköping University, Norrköping, Sweden.*
[6]*Stellenbosch Institute for Advanced Studies (STIAS), Wallenberg Research Center at Stellenbosch University, Stellenbosch, South Africa.*
[7]*Electrical Engineering Division, Department of Engineering, University of Cambridge, Cambridge, UK.*

Correspondence to G.G.M. and J.R.
gm603@cam.ac.uk; jrivnay@northwestern.edu

doi:10.1038/natrevmats.2017.86
Published online 16 Jan 2018

The invention of the transistor in 1947 heralded the era of microelectronics. Made of semiconductors, dielectrics and metals, the transistor enabled control of the flow of electrons in a solid-state device, thereby providing a robust alternative to vacuum tubes. Its miniaturization led to the development of the integrated circuit, which is at the heart of every modern electronic device. Modern transistors rely on field-effect doping; the number of mobile electrons (n-type) or holes (p-type) inside a semiconductor is modulated by a voltage applied to a metallic electrode, which is separated from the semiconductor by a thin insulating layer (the gate dielectric)[1]. Such devices are referred to as MOSFETs, which is short for metal-oxide-semiconductor field-effect transistors. Interest in organic electronic materials, and in particular their potential for low-cost fabrication over large areas, led to the development of organic field-effect transistors (OFETs)[2]. These devices use conjugated, semiconducting small molecules and polymers and offer an alternative to inorganic devices for applications in which facile processing on different substrates and tunable electronic properties are required. Steady progress over the past three decades has led to the systematic development of materials with mobilities well above those of amorphous silicon, combined with impressive stability[3,4]. The potential of OFETs has been demonstrated in a variety of applications, including pixel drivers for displays[5], bionic skin[6], stretchable transistors[7] and extremely sensitive chemical sensors[8] that are even able to withstand operation in saltwater[9].

The organic electrochemical transistor (OECT) was developed by Wrighton and colleagues[10] in the mid-1980s. An OECT consists of an organic semiconductor film that is in contact with an electrolyte, in which an electrode (the gate) is immersed (FIG. 1a). Metal electrodes, called the source and drain, establish contact with the organic semiconductor film and define the channel through which holes or electrons flow from the source to the drain. An OECT relies on ions that are injected from the electrolyte into the organic film, thereby changing its doping state and hence its conductivity[11]. The operation, which is described using the terminology of both electrochemistry and solid-state physics, is controlled by voltages applied to the gate (gate voltage, V_G) and to the drain (drain voltage, V_D), which are referenced with respect to the source electrode. The gate voltage controls the injection of ions into the channel and therefore the doping state (redox state in the language of electrochemistry) of the organic film. The drain voltage induces a current (drain current, I_D), which is proportional to the quantity of mobile holes or electrons in the channel, and therefore probes the doping state of the organic film. Like MOSFETs and OFETs, OECTs operate like a switch, in which the gate voltage (input) controls the drain current (output). They can also be viewed as an amplifier, in which the power of an input signal is amplified on the way to the output[12].

A typical material for OECTs is the conducting polymer poly(3,4-ethylenedioxythiophene) doped with poly(styrene sulfonate) (PEDOT:PSS). The semiconducting PEDOT is p-type doped (oxidized in the language of electrochemistry), which leads to mobile holes that can hop from one chain to another, resulting

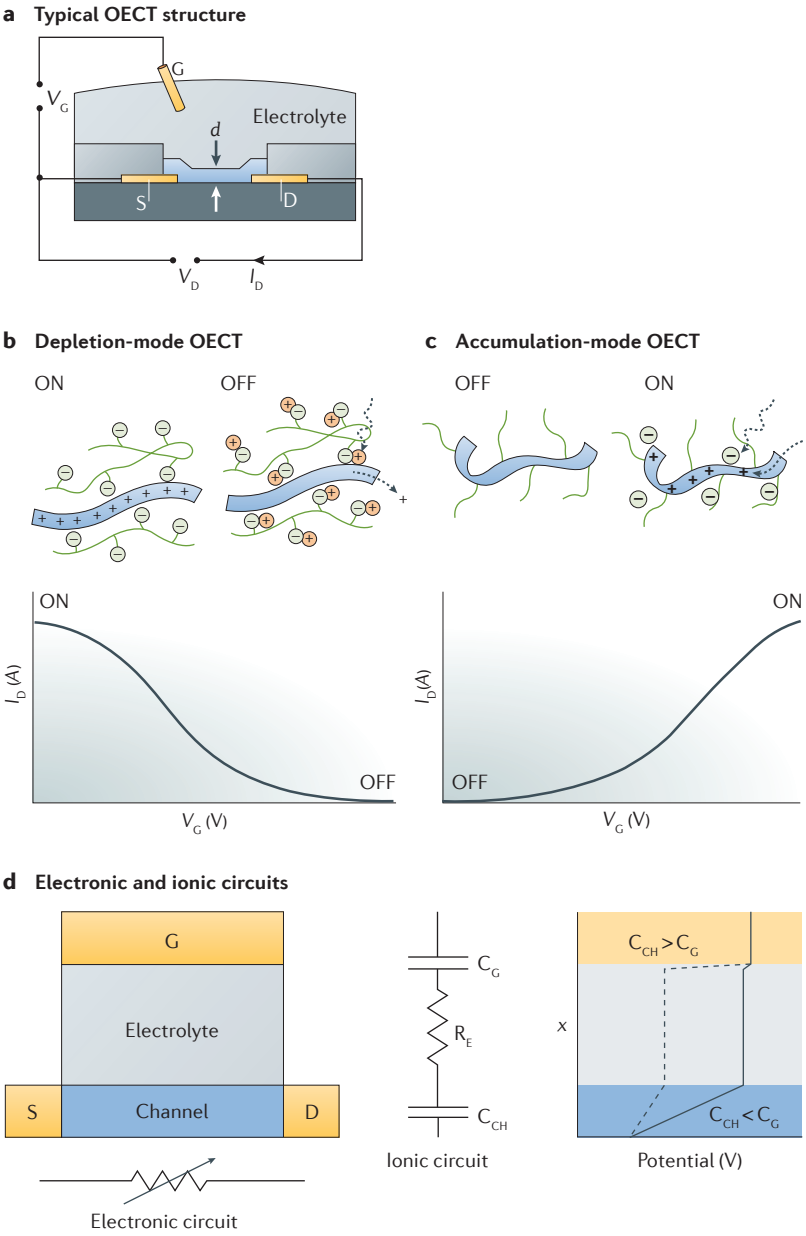

Figure 1 | **The device physics of organic electrochemical transistors. a** | The typical structure of an organic electrochemical transistor (OECT), showing the source (S), drain (D), electrolyte and gate (G). **b** | Transfer curve showing depletion-mode operation of an OECT with a conducting polymer channel. At zero gate voltage, holes on the conducting polymer contribute to a high drain current and the transistor is ON. When a gate voltage is applied, the holes are replaced by cations and the transistor is OFF. **c** | Transfer curve showing accumulation-mode operation of an OECT with a semiconducting polymer channel. At zero gate voltage, the channel has few mobile holes and the transistor is OFF. When a gate voltage is applied, holes accumulate and compensate injected anions, and the transistor is OFF. **d** | Ionic and electronic circuits used to model OECTs. The electronic circuit, shown below the device layout on the left, is modelled as a resistor with a resistance that varies upon gating. The ionic circuit, shown in the middle, consists of capacitors corresponding to the channel, C_{CH}, and gate, C_G, respectively, and a resistor corresponding to the electrolyte, R_E. The panel on the right shows the distribution of potential in the ionic circuit. The solid line corresponds to the case of efficient gating, in which most of the applied gate voltage drops at the electrolyte–channel interface, driving ions inside the channel. The dashed line corresponds to the case of poor gating, where most of the applied gate voltage drops at the gate–electrolyte interface. *d*, channel thickness; I_D, drain current; V_G, gate voltage; V_D, drain voltage; *x*, distance. Part **a** is adapted from REF. 177, Macmillan Publishers Limited.

in a hole current once a drain voltage is applied. These holes are compensated by the sulfonate anions of PSS, which in terms of solid-state physics can be considered as ionized acceptors[13]. OECTs based on conducting polymers, such as PEDOT:PSS, work in depletion mode. In the absence of a gate voltage, a hole current flows in the channel (that is, the ON state). Once a positive gate bias is applied, cations from the electrolyte are injected into the channel and the anions are compensated (FIG. 1b). This is equivalent to compensation doping, that is, implanting donors in p-type silicon. As a result, the number of holes in the channel decreases and the film is dedoped as the holes that are extracted at the drain are not replenished at the source. This leads to a drop in the drain current, and the device reaches the OFF state[11]. By contrast, accumulation-mode OECTs made of semiconducting polymers are normally in the OFF state owing to the small number of mobile holes in the channel (FIG. 1c). Application of a negative gate voltage causes injection of anions into the channel and a corresponding accumulation of holes (electrochemical doping in the language of electrochemistry), leading to the ON state[14].

The identifying characteristic of OECTs is that doping changes occur over the entire volume of the channel, as opposed to a thin interfacial region like in field-effect transistors (FETs) (BOX 1). Therefore, large modulations in the drain current can be achieved for low-gate voltages, which makes OECTs efficient switches and powerful amplifiers[12,15]. The use of electrolytes instead of MOS capacitors also allows for large flexibility in device architecture and integration with a variety of substrates, employing a variety of form factors and a broad range of fabrication processes. The inherent tunability of organic molecules further enables the optimization of ion and electron transport and facile biofunctionalization. Because of these features, OECTs are being explored for a wealth of applications, including neural interfaces[16,17], chemical and biological sensors[18,19], printed circuits[20,21] and neuromorphic devices[22,23]. In this Review, we discuss the physics of OECTs and the different organic materials used to make the devices, as well as outline the evolution of their technology, highlight various applications and take a critical look at the future of OECT research and development.

The device physics of OECTs

OECTs transduce small voltage signals applied to the gate into large changes in the drain current. This transduction process is described by a transfer curve, which shows the dependence of the drain current on the gate voltage (FIG. 1b,c). The steeper the transfer curve, the larger the change in drain current for a given gate voltage signal. The efficiency of transduction is calculated by the first derivative of the transfer curve, namely, transconductance $g_m = \partial I_D / \partial V_G$, which is an important figure of merit for transistors. OECTs possess very high transconductance values, on the order of millisiemens for micrometre-scale devices[12], which is attributed to the volumetric nature of their response.

An essential consideration in OECT physics is described by the Bernards model[11]. This model assumes

that ions from the electrolyte enter the channel and change the electronic conductivity throughout its volume, capturing the steady-state and transient response[11]. According to this model, the device is divided into two circuits: an ionic circuit, which describes the flow of ions in the gate–electrolyte–channel structure, and an electronic circuit, which describes the flow of electronic charge in the source–channel–drain structure according to Ohm's law (FIG. 1d). Therefore, the electronic circuit is treated as a resistor, in which electronic charge drifts under the influence of the local potential in a fashion identical to that of MOSFETs. The ionic circuit consists of a resistor, describing the flow of ions in the electrolyte, in series with a capacitor, describing the storage of ions in the channel. This model implies a purely capacitive process, according to which ions injected in the channel do not exchange charge with the organic film but rather electrostatically compensate the presence of opposite charges[24]. In this model, therefore, there are no electrochemical reactions between the electrolyte and the channel. At steady state, the capacitor is charged and the gate current goes to zero.

The Bernards model provides a good fit for the output characteristics of OECTs and allows quantitative predictions of the transconductance, g_m. At saturation and for depletion-mode devices, it gives[17]:

$$g_m = (W/L)\cdot d\cdot\mu\cdot C^*\cdot(V_{Th} - V_G), \quad (1)$$

where W, L and d are the channel width, length and thickness, respectively; μ is the charge-carrier mobility; C^* is the capacitance per unit volume of the channel; and V_{Th} is the threshold voltage. The voltage terms are reversed for accumulation-mode devices. This equation is similar to the one for FETs, with the difference that the product $d\cdot C^*$ replaces the capacitance per unit area of the MOS capacitor, C'. This variation defines the difference between the two devices. In a FET, the physical thickness of the channel does not enter the equation, whereas in an OECT, the channel thickness is a parameter that can tune the performance. For example, in a typical OFET with a 100 nm-thick SiO_2 layer, C' is in the tens of nF cm^{-2} (REF. 25). In OFETs gated with an electrolyte, the C' of the electrical double layer is of the order of 1–10 μF cm^{-2} (REFS 26,27). In an OECT with a 130 nm-thick PEDOT:PSS channel, the product of $d\cdot C^*$, which is the equivalent capacitance per unit area, is 500 μF cm^{-2} (REF. 17) (BOX 1). Therefore, volumetric gating gives OECTs a better performance in terms of amplification compared with other transistor technologies[12].

The high transconductance of OECTs comes at the cost of rather slow operation. The Bernards model predicts that the response time is limited by either the ionic or the electronic circuit[11]. In most devices, the ionic circuit dominates the response time, dictated by the product of the resistance of the electrolyte and the capacitance of the channel. The latter is proportional to the thickness of the channel; therefore, OECTs are slower as d increases. As a result, channel thickness can be used as a parameter to adjust the trade off between gain and bandwidth[17]. In practice, microfabricated OECTs with liquid electrolytes can achieve response times of a few tens of microseconds[12], limiting the scope to applications that require maximum frequencies in the range of tens of kilohertz. This is adequate for most biosensor applications, which are quasi-static, and for recording electrophysiological signals[28]. The use of gel or solid electrolytes leads to even slower response times, yet there are possibilities for application in areas such as printed electronics that do not require fast transistors[29].

The Bernards model offers a good starting point for understanding the basic physics of OECTs, but there are other considerations that have been or still need to be taken into account. For example, spatially resolved voltage measurements along the OECT channel imply that the conductivity along the channel varies with charge density in a nonlinear fashion[30]. Introducing a charge density-dependent conductivity in the Bernards model improves the quality of the output curve fitting of PEDOT:PSS OECTs[31]. Nonideal contacts in OECTS introduce additional complications[32]. A more accurate description of the transfer curve is achieved by considering the influence of disorder on hole transport in the channel[33]. Finally, OECTs represent the limit at which ions freely penetrate the volume of the channel. This has been demonstrated in several materials in which capacitance

Box 1 | **Organic-based transistors**

Field-effect transistors (FETs)

In a FET, an organic semiconductor film (the channel) is separated from a metal electrode (the gate) by a thin insulating layer (the gate dielectric). A voltage applied between the gate and the channel leads to field-effect doping of the semiconductor, that is, the accumulation of mobile electronic charge near the interface with the dielectric (figure, part **a**). The charge in the channel is compensated for by a sheet of charge at the gate electrode. The two sheets of charge form the two plates of a parallel plate capacitor. The amount of charge that is induced in the channel can be estimated by $Q = C\cdot V$, where C is the capacitance of the dielectric and V is the gate voltage. The capacitance is inversely proportional to the distance between the two plates. Therefore, thin dielectric layers maximize the amount of induced charge and thus the drain current of the transistor. In an electrolyte-gated FET, a double-layer capacitor is formed at the electrolyte–channel interface (figure, part **b**). A sheet of ionic charge in the electrolyte compensates the induced sheet of electronic charge in the channel. This configuration can be considered an extreme case of FET, because the thickness of the dielectric is reduced to dimensions on a par with the ionic radius, resulting in high capacitance.

Organic electrochemical transistors (OECTs)

In an accumulation-type OECT, ions penetrate the semiconductor, leading to changes in the doping state throughout the channel (figure, part **c**). This configuration is described not by a parallel plate capacitance but by a volumetric capacitance, which can be many orders of magnitude larger. Compared with a FET of similar size, the same gate voltage induces more electronic charge in the channel and thus a larger drain current in an OECT. Similary, high drain current can be achieved with depletion-type devices.

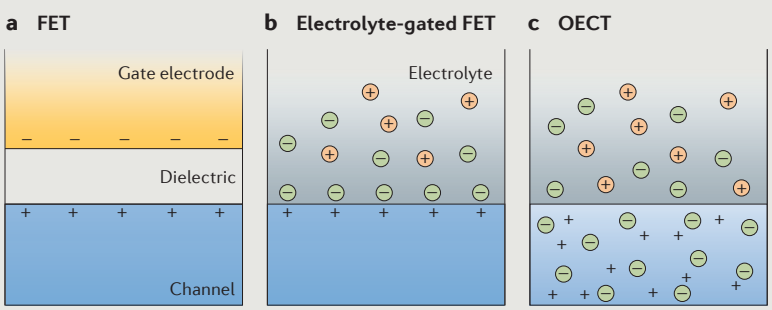

is found to be proportional to film thickness[14,17,34]. Electrolyte-gated FETs represent the other limit at which ions accumulate at the surface of the channel. Some materials show behaviour between the two limits[35,36], suggesting the presence of a barrier for ion injection. These observations point to an important fundamental issue. The physics of hole and electron injection and transport in organic semiconductors has been extensively studied over the past few decades, whereas little is known about the processes of ion injection and transport in organic semiconductors.

As a consequence of the gating through an electrolyte, OECTs have some specific characteristics. For example, the fraction of the applied gate voltage that drops across the channel is controlled by the nature and geometry of the gate electrode[37,38]. If a polarizable electrode, such as Pt or Au, is used as the gate, two capacitors are formed in the ionic circuit; one capacitor corresponds to the electrical double layer formed at the gate–electrolyte interface and the other corresponds to the volumetric capacitance of the channel. Because the capacitors are in series, the applied gate voltage drops across the smaller capacitor (FIG. 1d). For efficient gating, the capacitance of the gate electrode must be more than ten times larger than the capacitance of the channel, otherwise a large fraction of the applied gate voltage will drop at the gate–electrolyte interface (FIG. 1d). Such large gates can be technically difficult to implement for some applications; however, using a thick PEDOT:PSS electrode as the gate can help achieve a large gate capacitance. Alternatively, a nonpolarizable gate electrode, such as Ag/AgCl, can be used. In this case, the voltage drop at the gate–electrolyte interface is negligible[39], and effective gating is achieved. However, it should be noted that in some sensing applications, a small gate electrode is preferable, for example, when a sensing reaction is meant to occur at the gate and the channel merely acts as the transducer[40]. Finally, the nature of the electrolyte, liquid, gel or solid and the ion concentration influence the response time of the transistor because the electrolyte conductivity determines the resistor of the ionic circuit[41].

Materials for OECTs

The channel of OECTs is typically made of a conducting polymer, most commonly PEDOT or polypyrrole (PPy), doped with p-type dopants such as small anions or polyanions (FIG. 2a,b). These materials are synthesized by solution, vapour-phase or electrochemical polymerization. By far, the most popular material is PEDOT:PSS, which has been explored for a great variety of applications over the past 15 years, owing mainly to its commercial availability in the form of aqueous dispersions, which permits the facile deposition of thin films using solution-processing techniques[13]. The dispersions are prepared by polymerizing EDOT, the monomer of PEDOT, in the presence of PSS. Films of PEDOT:PSS cast from these dispersions show high electronic[13] (hole) conductivity and are widely used in electrostatic coatings and as anodes for light-emitting diodes and solar cells[13]. As a consequence, the structure and electronic conductivity of these films have been thoroughly investigated[42,43]. Various co-solvents, surfactants and processing methods have been used to maximize hole conductivity, which is currently in excess of 1,000 S cm^{-1} (REF. 44). Electrochemical moving-front measurements revealed that small ions are injected from an electrolyte into PEDOT:PSS films in a barrierless fashion and have drift mobilities close to those in bulk water[45–47]. Finally, PEDOT:PSS films show good electrochemical stability in aqueous electrolytes[48] and can be rendered insoluble in water through the addition of crosslinkers such as (3-glycidyloxypropyl)trimethoxysilane[49,50] and divinylsulfone[51]. Overall, it is technically rather simple to make PEDOT:PSS OECTs with a transconductance in the range of millisiemens and a response time in the range of tens of microseconds[12], which makes devices based on this conducting polymer suitable for the vast majority of the applications pursued for OECTs.

Despite the attractive properties and good performance of PEDOT:PSS in OECTs, these films have some limitations. More specifically, the structure of PEDOT:PSS is complex, which limits its use as a model system for structure–function relationships. Also, in terms of electrical properties, the bulky structure of PSS affects the volume fraction of PEDOT in the film and hence the volumetric capacitance[24]. For this reason, conjugated polymer motifs with higher hole mobility than PEDOT, such as ones that rely on fused thiophenes, have been developed[52]. In terms of mechanical properties, Young's modulus of PEDOT:PSS is considerably higher than that of most biological tissues[49,53], which can be a limitation for applications in bioelectronics. Moreover, although PEDOT:PSS films are broadly cytocompatible[54], polymers or composites allowing more versatile biofunctionalization are desirable. Finally, in terms of solution processing, the acidity of PSS can cause corrosion of the print heads. These limitations motivate researchers to synthesize new materials for OECTs.

Replacing PSS with less acidic polyanions, such as polymers containing (trifluoromethylsulfonyl)imide side groups, results in OECTs with a similar performance in terms of transconductance and response time as PEDOT:PSS-based OECTs[55]. A different approach involves removing PSS and instead attaching ionic groups directly on the thiophene backbone through side chains. Such conjugated polyelectrolytes are semiconducting when the ion is compensated by a counter ion (FIG. 2c) or conducting when compensated by an electronic charge on the conjugated backbone (FIG. 2d). For example, accumulation-mode OECTs with a transconductance of the order of millisiemens have been developed using a semiconductor based on a polythiophene with a sulfonate group attached to the backbone with a hexyl chain (PTHS)[56] (FIG. 2c). Depletion-mode OECTs have been designed using a conductor based on PEDOT with a pendant sulfonate group (PEDOT-S)[57] (FIG. 2d). Blending a semiconducting and a conducting conjugated polyelectrolyte yields OECTs that can be tuned by balancing the stoichiometry of the channel[57]. Alternatively, conjugated polymers with hydrophilic or ion-transporting side chains can be used as OECT materials. OECTs made from poly(2-(3,3′-bis(2-(2-(2-methoxyethoxy)

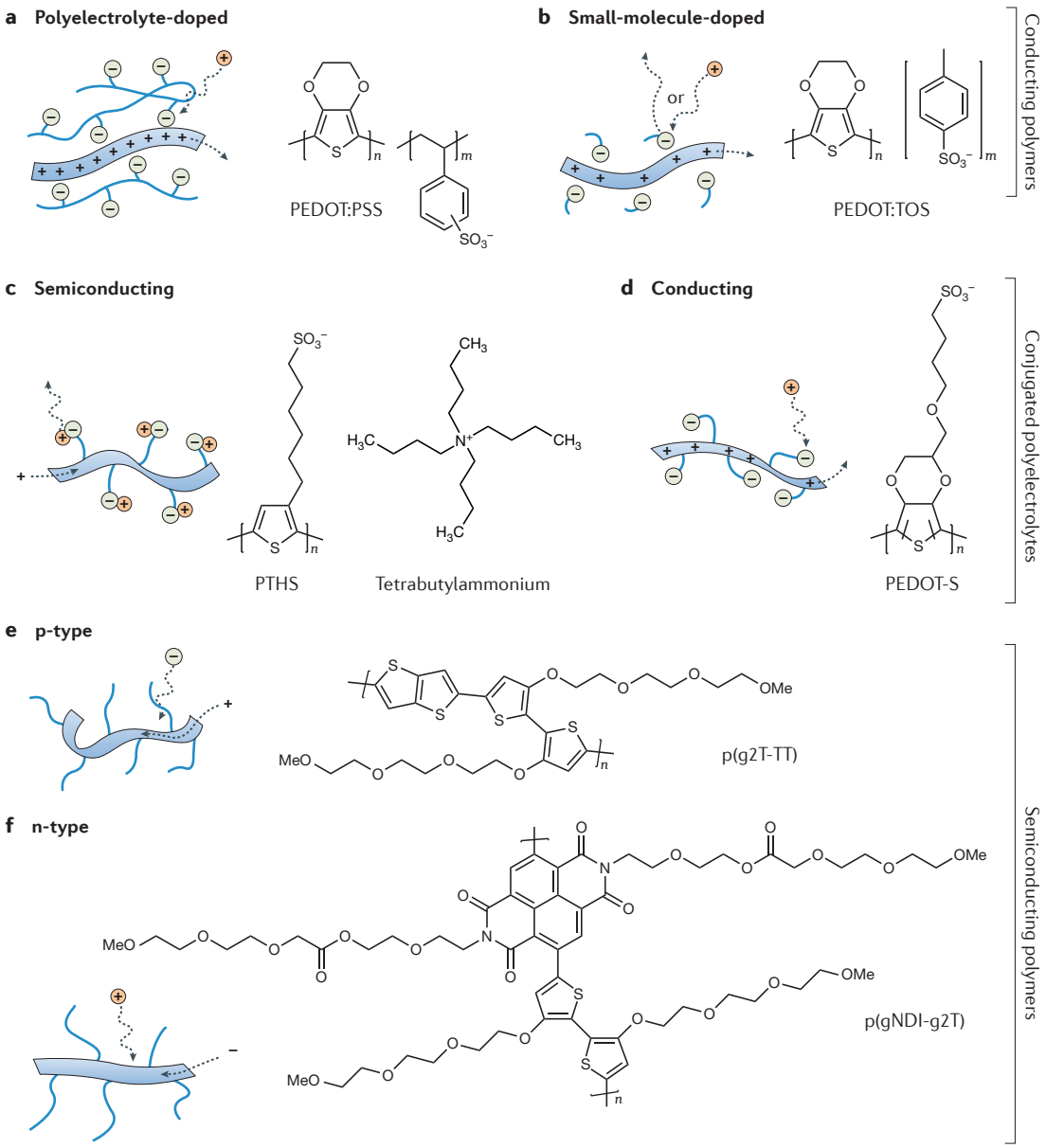

Figure 2 | **Different classes of materials used in organic electrochemical transistor channels.** Conducting polymers include poly(3,4-ethylenedioxythiophene) doped with poly(styrene sulfonate) (PEDOT:PSS) (part **a**) and poly(3,4-ethylenedioxythiophene) doped with tosylate (PEDOT:TOS) (part **b**). In these materials, holes (represented by plus signs) on the PEDOT backbone are compensated by anions (green circles). Dedoping takes place through the injection of cations (orange circles) or extraction of anions, accompanied by extraction of holes, as indicated by the arrows. Conjugated polyelectrolytes include semiconducting poly(6-(thiophene-3-yl)hexane-1-sulfonate) tetrabutylammonium (PTHS) (part **c**) and conducting poly(4-(2,3-dihydrothieno[3,4-b][1,4]dioxin-2-yl-methoxy)-1-butanesulfonic acid) (PEDOT-S) (part **d**). Doping and dedoping mechanisms are indicated by arrows. Semiconducting polymers include p-type poly(2-(3,3′-bis(2-(2-(2-methoxyethoxy)ethoxy)ethoxy)-[2,2′-bithiophen]-5-yl)thieno[3,2-b]thiophene) (p(g2T-TT)) (part **e**) and n-type poly((ethoxy)ethyl 2-(2-(2-methoxyethoxy)ethoxy)acetate)-naphthalene-1,4,5,8-tetracarboxylic-diimide-co-3,3′-bis(2-(2-(2-methoxyethoxy)ethoxy)-(bithiophene)) (p(gNDI-g2T)) (part **f**). These polymers can be doped by the injection of ions, as indicated by the arrows.

ethoxy)ethoxy)-[2,2′-bithiophen]-5-yl)thieno[3,2-b] thiophene) p(g2T-TT), a polythiophene with glycolated side chains, exhibit better transconductance values than PEDOT:PSS-based OECTs of the same geometry[36] (FIG. 2e). Using the same side-chain functionalization, an n-type copolymer poly((ethoxy)ethyl 2-(2-(2-methoxyethoxy) ethoxy)acetate)-naphthalene-1,4,5,8-tetracarboxylic-diimide-co-3,3′-bis(2-(2-(2-methoxyethoxy)ethoxy) ethoxy)-(bithiophene)) p(gNDI-g2T), based on naphthalene-1,4,5,8-tetracarboxylic diimide and bithiophene units, was used to design ambipolar OECTs with high stability during pulsed measurements over 2 hours in aqueous media[34] (FIG. 2f). Finally, the blending of

PEDOT:PSS with poly(vinyl alcohol) (PVA) provides a handle for subsequent silanization, allowing for the covalent linkage of biological moieties onto the films without any deleterious effects on the electrical properties[58]. It has been demonstrated that these films can be functionalized with polypeptides and proteins that maintain their biological activity.

Electrochemical polymerization is a versatile method for incorporating biomolecules in conducting polymers[59] and was used to fabricate the first OECT[10]. However, the method has fallen out of favour because it relies on growth from a conducting surface, which is hard to implement in OECTs. An alternative method, vapour-phase polymerization, can also incorporate different biomolecules in the channel of OECTs. In this process, a film cast from a precursor solution containing tosylate (TOS, the pendant group of PSS) moieties is exposed to EDOT vapour to yield the conducting polymer PEDOT:TOS[60] (FIG. 2b). The mixing of different polymers in the precursor solution results in high-quality composites. Indeed, composites of PEDOT:TOS with polyethylene glycol (PEG) have OECT performance similar to that of pristine PEDOT:TOS[61]. The use of a carboxyl-containing PEG demonstrates the potential of vapour-phase polymerization in applications requiring biofunctionalization. Furthermore, gelatin, which is the denatured form of the extracellular matrix protein collagen, can be incorporated into PEDOT:TOS without altering the electrochemical properties of the conducting polymer or its performance in OECTs[62]. Such composites were found to support bovine brain capillary endothelial cell adhesion and growth *in vitro*, indicating a functional protein. Finally, vapour-phase polymerization can be applied to produce PEDOT:TOS composites with poly(tetrahydrofuran), which show a hysteresis effect in their OECT characteristics[63]. The hysteresis is attributed to a conformational change in the polymer during redox cycling and was used to demonstrate a nonvolatile memory device.

A variety of electrolytes, including gels[64] and solids[65], and the use of different gate electrodes, including traditional polarizable electrodes (such as Pt)[66] and non-polarizable electrodes (such as Ag/AgCl[66]) as well as non-traditional materials (such as PEDOT:PSS[65] and various forms of carbon[67,68]), have been used to fabricate OECTs. The choice of material is often dictated by the application or limitations imposed by fabrication. To test new channel materials, the components commonly used are prepatterned Au source and drain electrodes on a glass substrate, a Ag/AgCl gate electrode and an aqueous solution of NaCl or KCl as the electrolyte.

The history of OECT technology

In 1980, the first indirect measurements of the reversible electrochemical switching of electronic conductivity in polypyrrole, recorded from films made on Pt electrodes, were reported[69]. A few years later, polypyrrole films electropolymerized onto Au, separated by 1.4 µm gaps on SiO_2-coated Si wafers, were shown to extend and even bridge the gaps between electrodes[10]. This device had the action of an accumulation-mode transistor, which was recorded using a two circuit drain–source and a gate–counter–reference electrode probing approach. Since then, different probing setups and other polymers, such as polypyrrole, poly(3-methylthiophene)[70] and polyaniline[71], have been applied as the active layer in electrochemical transistors for redox sensing and chemiresistor applications[72]. In addition, several OECTs based on microfabricated lateral electrodes on rigid substrates have been reported (FIG. 3a). Specifically, advances have included the fabrication of sandwich structures[73], the incorporation of solid electrolytes[74,75], the use of channels that incorporate diaphorase enzymes[76] and the demonstration of high performance in aqueous and nonaqueous electrolytes[77].

The use of electrolytes as gating media allows for great flexibility in OECT design in terms of placement of the gate electrode with respect to the channel. Moreover, 'long-channel' effects can be addressed. In OFETs, charges are transported along the thin sheet of accumulated holes or electrons, residing at the semiconductor–gate dielectric interface. In a long channel, this typically results in very low currents, preventing the use of OFETs as drivers for power consuming components. This is particularly problematic in all-printed systems, where only long channels can be manufactured with high yield. By contrast, in OECTs, the entire bulk contributes to charge transport; thus, higher currents can be supplied for the same given channel length. Therefore, different designs of OECTs with low operating voltage can be fabricated with respect to gate, electrolyte, channel dimensions and relative positions. Additionally, different deposition and patterning techniques on a variety of substrates, including flexible and stretchable substrates, can be applied, paving the way for drastically new device architectures and form factors (FIG. 3b).

The first electrochemical transistor that was, in part, manufactured using printing techniques was reported in 1994 (REF. 78). Carbon-based source and drain electrodes and dielectrics were screen-printed on a polyvinyl chloride base, and the assembled structure was then cracked in liquid nitrogen. Polyaniline was anodically grown along the fractured edge and coated with glucose oxidase (GOx) immobilized in poly(1,2-diaminobenzene). The resulting device, with a channel length and width of 20 µm and 4.5 mm, respectively, was used as a microelectrochemical enzyme transistor for glucose[79] and peroxide sensing[80]. An OECT with a channel length of 0.5 mm gated through a thick filter paper soaked with 1 M KCl electrolyte was also reported[81].

In the early 1990s, PEDOT was explored as an electronic ink and coating for a wide range of conductive, electronic and electrochemical applications[82–84]. When combined with the dopant PSS, PEDOT shows good redox stability and high electronic conductivity, and can be incorporated into high-performing OECT structures. Using printing techniques, devices in which PEDOT:PSS serves as both the active channel and the electrode for the gate, drain and source are possible. A decade later, the *in situ* redox switching of the electronic conductivity in PEDOT was explored using different electrochemical setups and device configurations, such as electrochromic pixels[85,86]. In 2002, the first demonstrations of transistors

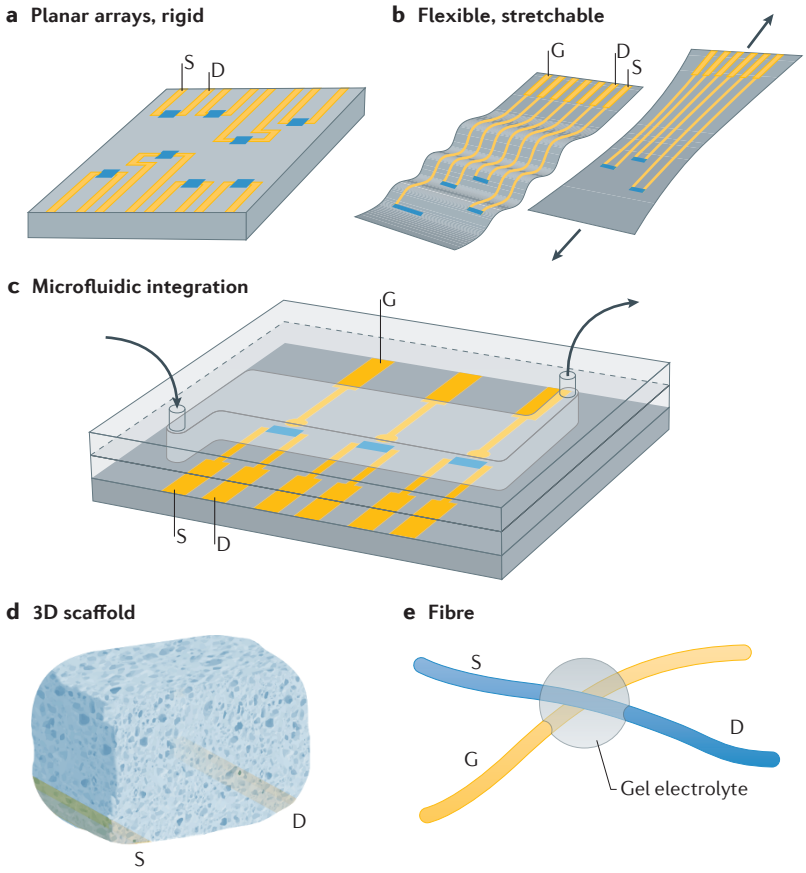

Figure 3 | **Form factors of organic electrochemical transistors.** Organic electrochemical transistors (OECTs) are available in a variety of form factors, including planar devices on rigid substrates (part **a**), devices that are flexible and stretchable (part **b**), devices that are integrated with microfluidics (part **c**), devices with channels in the form of 3D scaffolds (part **d**) and devices made of fibres (part **e**). D, drain; G, gate; S, source.

with PEDOT were reported[65,87,88]. For example, by deactivating or patterning PEDOT:PSS coatings using screen printing, an all-laterally configured gate, drain and source OECT with a screen-printed gelled electrolyte on top could be realized[87]. In such lateral OECTs, drain current ON/OFF ratios of 10^5, a transconductance of 1.2 mS and a maximum frequency operation of 200 Hz can be achieved.

Easy manufacturing protocols for high-performing and low operating-voltage OECTs sparked the development of various OECT structures that are based on PEDOT:PSS and other mixed ionic–electronic polymer conductors as well as the development of related high-volume manufacturing processes. Lateral PEDOT:PSS-based OECTs can be combined with vertical electrochromic display cells and manufactured by printing techniques on coated paper to form actively addressed smart pixels and displays[89]. Long PEDOT:PSS channels enable integration and gating through microfluidic systems made from polydimethylsiloxane (PDMS)[90] (FIG. 3c), a technology that also facilitates OECT gating through a phospholipid membrane[91] and through cells[92]. Polyaniline, PPy and PEDOT nanowires can be grown between Pt source and drain electrodes and remotely gated through an electrolyte[93]. OECTs were also developed using 3D porous sponges of PEDOT:PSS, a form factor of interest for tissue culture applications[94] (FIG. 3d).

Paper and plastic foils are among the largest surfaces ever manufactured and therefore have attracted great attention from the OECT community. Several approaches to standard and modified printing techniques have been explored to produce OECT devices and circuits along those surfaces, such as screen printing[95] and inkjet printing[96]. All-screen-printed OECT logic circuits, such as flip flops and shift registers operating at 1.5 V, have been achieved on poly(ethylene terephthalate) (PET) substrates[21]. An ultrathin carrier, made on a 4 µm-thin parylene sheet, for OECTs has been explored in bioelectronic applications[16]. Textiles are also an attractive carrier for OECTs, with potential applications in the field of wearable electronics. For example, PEDOT-based transistors have been made on Gore-Tex as gas sensors on 'breathable' substrates[97] and have also been screen-printed on common fabrics, such as woven cotton and Lycra, to serve as wearable sensors for the sensing of external biological fluids, for example, sweat, saliva and urine[98].

Paper and textiles are made of fibres, and several approaches have been explored to build OECTs and even complex circuits on individual or combinations of fibres[99] (FIG. 3e). For example, OECTs based on PPy made on a nylon nanofibre can be explored for lead-ion detection[100], and PEDOT:PSS soaked into natural cotton fibres can be used to form an OECT channel for saline sensing[101]. PEDOT:PSS has also been explored in combination with nanofibrillated cellulose (NFC) as a cladding layer around the fibres. This combination provides a scalable technology for self standing and large-scale OECT systems, for instance, a reconfigurable OECT sticker platform[102]. A transconductance beyond 1 S has also been demonstrated in PEDOT:PSS–NFC OECTs[103]. Finally, a unique form factor has been achieved by making OECTs from PEDOT derivatives that are infused into living plants[104]. Such OECTs are envisioned to monitor and control plant development in the future.

Applications of OECTs

Bioelectronics

Organic electronic materials and OECTs have a major role in various bioelectronic devices for health care-related uses and biomedical research[54,105,106]. In electrophysiology, OECTs are interfaced with electrically active tissues and organs to measure cell activity (FIG. 4a). For example, microfabricated PEDOT:PSS OECTs on parylene substrates can be placed on the brain of a rat to record epileptic seizures. The signal-to-noise ratio of such recordings is over 20 dB higher than that of PEDOT:PSS electrodes[16], and, owing to local signal amplification, activities from deep brain tissue can be recorded. As a consequence of the direct and oxide-free contact between the conducting channel and cerebrospinal fluid, OECTs can also be used to locally inject current and stimulate neurons[107]. OECTs that are integrated with organic thin-film transistors are capable of

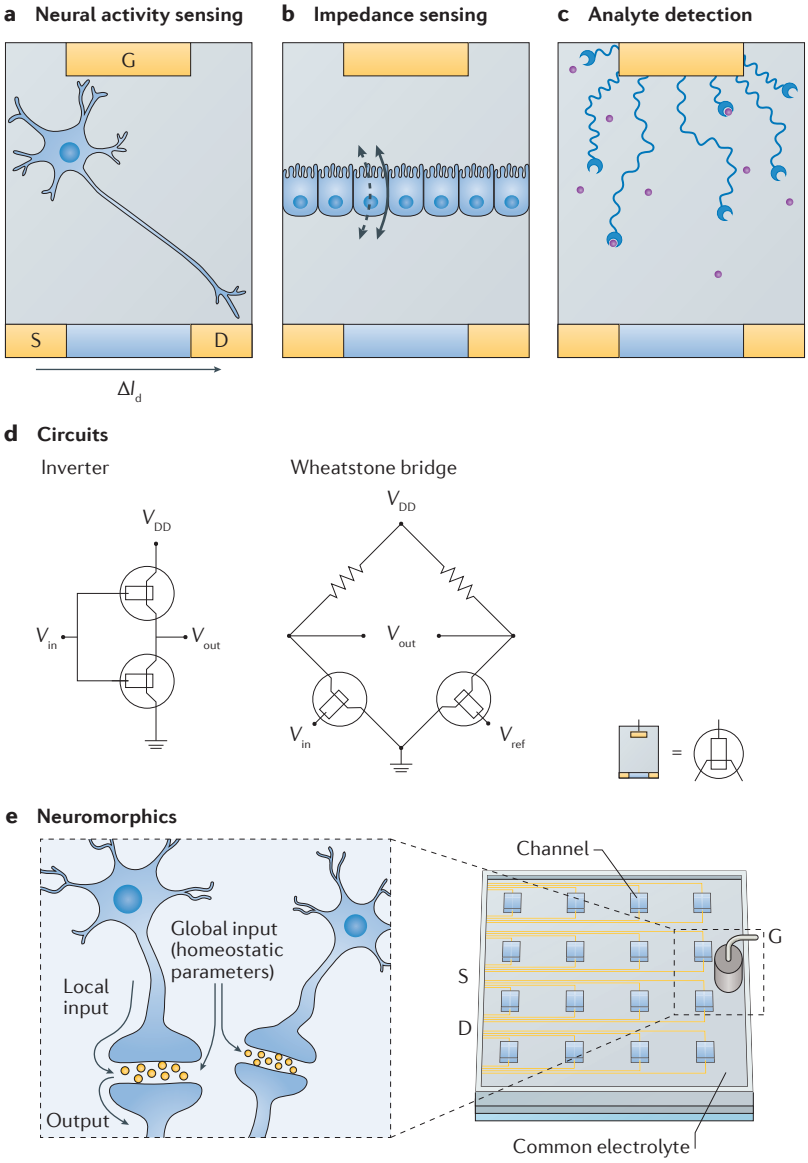

Figure 4 | **Applications of organic electrochemical transistors.** Organic electrochemical transistors (OECTs) are used in electrophysiology to record the electrical activity of cells, such as neurons, in the electrolyte between the channel and the gate (part **a**). They are also used as impedance sensors that record changes in ion permeability of cell layers placed between the channel and gate (part **b**) and for the detection of analytes (red circles) that interact with receptors placed at the gate or channel (part **c**). In all these cases, the detection of an event is signalled by a change in the drain current, ΔI_d. A variety of circuits, including inverters and Wheatstone bridges (part **d**), have been developed to process an input voltage signal V_{in} to an output voltage signal V_{out}. OECTs can also be used as devices that mimic features of biological neural networks, such as the ability to control an entire network through a global signal (part **e**). D, drain; G, gate; S, source; V_{DD}, supply voltage; V_{ref}, reference voltage.

recording myograms in transgenic rats with high temporal resolution[108]. Cutaneous applications are also being explored. For example, OECTs can record an electrocardiogram when placed on human skin[109]. OECTs can further amplify recordings of electrophysiological signals from the human brain, heart and muscle[17,110,111]. Finally, PEDOT:PSS OECTs can be sterilized by autoclaving, paving the way for clinical applications[112].

OECTs can also be used in conjunction with cell cultures for drug screening. For example, OECT arrays can record action potentials from cardiomyocytes with excellent signal-to-noise ratio[113] and provide a spatial map of the electrophysiological activity[114]. OECTs can also be used to monitor cell coverage[115], barrier tissue formation and cellular health[116–120] for nonelectrogenic cells, such as epithelial cells (FIG. 4b). Most of these measurements involve the growth of a monolayer of cells between the channel and the gate, which introduces a barrier for ion motion in the electrolyte and therefore alters the characteristics of the OECT[121]. The same principle can be applied to study ion channels in supported lipid bilayers assembled on PEDOT:PSS channels[122]. Measurement protocols have been developed, using AC modulations[123] or white noise[124] applied at the gate, in which OECTs show superior performance compared to impedance sensing using electrodes. Given the optical transparency of PEDOT:PSS in the visible part of the spectrum, a key advantage of OECT devices is the possibility of simultaneous optical and electronic readouts[125]. Another advantage is that they work in complex environments, such as milk, where they were used for the detection of enteric pathogens by measuring transepithelial ion flow[126]. OECTs have also been applied to 3D cell culture models; for example, OECTs can be integrated with cyst-like 3D cultures to monitor their integrity and the effect of toxic compounds on the cell structure[127]. Finally, it should be mentioned that the arrangement of epithelial cells on an OECT channel can be controlled by the applied drain and gate voltage[128]. This offers the opportunity to not only monitor but also control cell behaviour. To this end, OECTs fabricated using porous sponges of PEDOT:PSS were able to host and control 3D cell cultures[94].

OECTs can also act as transducers in biosensors for the detection of electrolytes and metabolites, such as glucose and lactate, which are important for human health and performance monitoring (FIG. 4c). A variety of approaches have been developed to gain selectivity in ion detection[129,130]. For the detection of metabolites, the principle of sensor operation relies on the selective interaction of a redox enzyme with the metabolite and the consequent transfer of an electron to the gate of the OECT. The resulting change in the drain current depends on the concentration of the metabolite[40]. Initially, the enzyme is entrapped in the channel[79] or dissolved in the electrolyte[131]. Immobilization of the enzyme on the gate electrode then leads to the development of highly selective and sensitive sensors[132,133]. The combination of OECTs with microfluidics paves the way for multi-analyte sensor platforms[134,135], whereas combination with textiles allows for their use in wearable applications, for example, for the detection of analytes in sweat[98,136].

Although many applications of OECTs have focused on analyte detection in saline solutions, examples of sensing in breath[137], sweat[138], saliva[139] or cell culture media[140] have also been demonstrated. These demonstrations make OECTs clinically relevant, as exemplified by the use of OECT lactate sensors to measure

the metastatic potential of tumour cells[140]. Moreover, OECTs provide an easy way to amplify fast-scan cyclic voltammetry, allowing for simpler instrumentation compared to commercially available tools[141]. For example, OECTs enable the selective detection of dopamine in the presence of interfering compounds, with sensitivities and limits of detection comparable to, or better than, those obtained using sophisticated electrochemistry techniques such as differential pulse voltammetry[142]. Similarly, the highly sensitive detection of adrenaline with OECTs has been reported[143]. Finally, in separate studies, OECTs have been shown to be suitable for the sensing of DNA[144] and bacteria[145].

Circuits and logic

The high transconductance and ON/OFF ratios along with low-voltage operation have encouraged scientists to incorporate OECTs in circuits (FIG. 4d). However, the relatively low switching speed compared to MOSFET technology prevents their application in (digital) signal processing and computation. Nevertheless, combining OECTs with silicon-based integrated circuits offers many promising opportunities, for example, providing internet connectivity in electronic label and skin-patch applications[146]. The first step in demonstrating operational OECT circuits was taken in 2002, when OECTs were included as pixel drivers in an active-matrix electrochromic display printed on paper[89]. PEDOT:PSS OECT circuits have also been explored to improve the matrix display fill factor[147] and to achieve negative-AND (NAND) and NOR gates[20]. Textiles and wire configurations, in addition to paper and plastic foils, represent an important large area and flexible platform for OECTs, where the fibre grid can potentially serve as a template or as an integral part of devices to connect and define circuits. Woven OECT logic circuits[99], NOR gates and inverters, using parallel PEDOT:PSS-based fabric wires combined with a polyelectrolyte, have already been achieved[148]. Similar to display pixels, sensor and detector devices can be arranged in matrices to enable spatially resolved sensing or detection. In such devices, OECTs can serve as the addressing switch or line and row driver to facilitate the *x*-*y* addressing of individual sensors in a crosspoint matrix. In an effort to achieve a touchless control interface, OECTs were printed and integrated to form addressing columns and readout rows for a ferroelectric sensor matrix[149].

Analog and logic OECT circuits have been realized for a variety of applications using different large-area and high-volume manufacturing techniques, such as screen printing[21,150], lamination[147], nanoimprinting[151], combined inkjet printing and vapour-phase polymerization[152]. A tenfold increase in sensitivity can be achieved using a PEDOT:PSS-based signal-ON sensor circuit, compared with a single OECT sensor[153]. Such sensor circuits can be applied for metabolite detection; for example, a Wheatstone bridge consisting of two PEDOT:PSS-based OECTs can be used for lactate sensing[140]. A voltage amplifier, combining a high-transconductance OECT with a resistor, enables improved recordings of electrocardiographic signals compared with electrodes[111]. Supercapacitor and energy-storage technology constitute other potential areas for the use of electrolyte-based devices. In energy-storage modules, several capacitors are typically included, with the need for high-transconductance switches to balance charging and discharging. An OECT-based differential amplifier was manufactured to balance and limit the voltage across capacitors to 1 V (REF. 150).

Memory and neuromorphic devices

There is great interest in developing device networks involving the co-location of computation and memory because of their efficiency in learning specific tasks, such as pattern recognition[154–156]. These systems are termed neuromorphic because they mimic the structure and function of the nervous system. Neuromorphic systems rely on devices that display temporary or permanent changes in electrical properties, thereby simulating short-term or long-term memory. Ions in OECTs can change the electrical state of the channel; therefore, a variety of memory and neuromorphic devices have been developed based on OECTs (FIG. 4e). For example, in an adaptive device based on a polyaniline channel and an electrolyte based on LiCl in poly(ethylene oxide)[157], hysteresis during a voltage sweep gives rise to bistable operation, which imparts a dependence of the channel resistance on the history of the device. Programmed states are stable for timescales of ~1,000 s (REF. 158). Follow-up work explored the integration of these devices in neural network architectures[159]. Devices using different electrolytes[160] and channel materials[161,162] were evaluated.

In general, an attractive feature of neuromorphic devices is their potential for low power consumption per switching event. This was demonstrated in devices based on polymer nanofibres that exhibit energies as low as 1.23 fJ per synaptic spike[163]. The first neuromorphic transistor based on a PEDOT:PSS OECT was described in 2015, and neuromorphic functions, such as paired-pulse depression, adaptation and dynamic filtering, were demonstrated[22]. The retention time can be further increased from a few seconds to several hours by replacing PEDOT:PSS with a modified polymer that undergoes a conformational change upon charging[164]. A system using multiple gates to modulate a single channel is able to discriminate the orientation of voltage patterns imposed on the gate electrode array, emulating the orientation selectivity of the mammalian visual system[165]. Another system using multiple channels and a single gate imitates homeostatic plasticity functions of the brain[166]. A different architecture for an organic neuromorphic device combines a battery[167,168] and an OECT. This design allows the inclusion of over 500 distinct synaptic states in a narrow (<1 V) voltage range and ensures that the programmed states change by less than 0.1% over tens of hours[23]. Finally, a ferroelectric polymer layer, coated on the gate electrode, can be used to control the redox state of a PEDOT:PSS channel[169]. Polarization switching of the ferroelectric polymer, which takes place once the coercive field is overcome, introduces a bistability that implements memory functionality.

Outlook

OECT research is at the intersection of materials science, solid-state physics, electrochemistry and electrical engineering. Although the Bernards model describes the physics of OECTs, it still needs refinement to better understand and optimize device operation. For example, the lateral motion of ions inside the channel has to be considered, which requires the development of 2D drift or diffusion models with appropriate boundary conditions at the electrolyte–channel interface. On a more fundamental level, although electronic charge injection at metal–organic interfaces has been well studied[170,171], little is known about ion injection from electrolytes into organic semiconductors owing to the difficulty in measuring ion injection and transport in the presence of electronic charge[45]. These processes are expected to be sensitive to the microstructure of the polymer and therefore should be analysed at a microscopic level[172]. Moreover, charge transport in OECT channels is complex[173,174] owing to the presence of water, high charge densities and dopants. For example, the effect of a large amount of water on the density of states of organic semiconductors remains elusive. However, computational methods that could answer this question are within reach. Finally, the development of simulation program with integrated circuit emphasis (SPICE) models is expected to greatly boost the design of OECT-based circuits[175,176].

Polymers with better performance than PEDOT:PSS are being developed. However, the lack of structure–function relationships hinders the rational design and synthesis of new materials. The development of *in situ* and *operando* measurements that combine structural, spectroscopic and electrical properties is particularly important because the film structure changes upon immersion and operation in an electrolyte environment[46,47,172]. Material properties need to be adapted to the purpose, environment and operational lifetime of a given device and application. For example, a stability of several weeks in aqueous electrolyte is a primary consideration for cell culture-based diagnostics, whereas a stability of a few minutes might be adequate for disposable sensors. Biocompatibility is crucial for implantable devices but not for memory-storage devices. Reversibility of the drain current through repeated gate pulses is highly desirable for most circuit and sensing applications, whereas hysteretic behaviour through trapping and retention of ions, and morphology changes in the channel allows for applications in memory and neuromorphic devices. Finally, the possibility to tailor ion selectivity paves the way for the development of different biosensors.

A consideration for materials design that is critical for all applications stems from the fact that the channel of an OECT must perform two tasks: transport electronic charge (measured by μ) and store ionic charge (measured by C^*). According to Equation 1, the figure of merit of the material is defined by the product of the charge-carrier mobility and volumetric capacitance ($\mu{\cdot}C^*$). For example, PEDOT:PSS with ethylene glycol has a $\mu{\cdot}C^*$ of 75 F cm^{-1} V^{-1} s^{-1} (REF. 17), whereas p-type materials, such as p(g2T-TT) (FIG. 2e), achieve

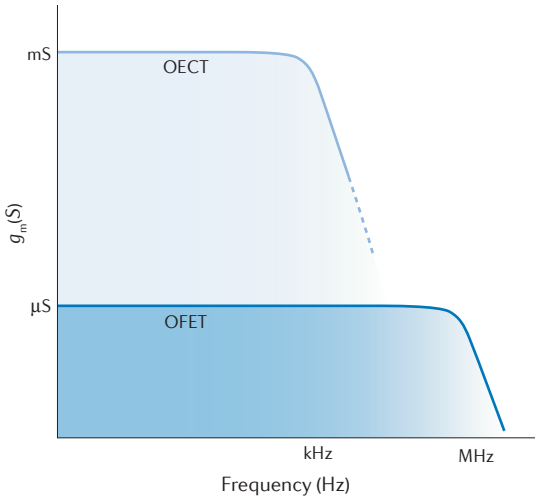

Figure 5 | **Comparison between organic electrochemical transistors and organic field-effect transistors.** The two devices are compared from the perspective of gain versus bandwidth. Typical organic electrochemical transistors (OECTs) show a transconductance, g_m, in the range of millisiemens, but g_m starts to roll off for frequencies higher than 1 kHz. Organic field-effect transistors (OFETs) show a lower transconductance, but they can be operated at higher frequencies. The area under the pale blue curve indicates the frequency range in which OECTs have a performance advantage.

a $\mu{\cdot}C^*$ of 228 F cm^{-1} V^{-1} s^{-1} (REF. 36). By contrast, n-type materials, such as p(gNDI-g2T) (FIG. 2f), have a $\mu{\cdot}C^*$ of ~0.1 F cm^{-1} V^{-1} s^{-1} (REF. 34). Decoupling the charge-carrier mobility and volumetric capacitance can explain why one material outperforms the other[177]. For example, p(g2T-TT) has a higher $\mu{\cdot}C^*$ than PEDOT:PSS because of a six times higher volumetric capacitance, but has a comparable hole mobility. p(gNDI-g2T) has the highest reported C^* (~400 F cm^{-3}), but low electron mobility (~1×10^{-4} cm^2 V^{-1} s^{-1}). A rule emerging from available materials is that even minimal hydrophilicity encourages ion transport and therefore is a requirement for OECT materials[14,34,36,45,178]. However, hydrophobic self-doped conjugated polyelectrolytes[179] and poly(3-hexylthiophene) have also been used as channel materials in water-based OECTs[172]. Additionally, block copolymers or blends of semiconducting and ion-conducting polymers allow for the separate control of ion and electron transport[180], which makes them interesting for OECTs. Finally, small molecules are envisioned to play a key role in the development of OECTs with tunable structure–function relationships.

OECTs have great design flexibility and can be manufactured by a variety of fabrication techniques, leading to different form factors compatible with low-cost, flexible, large-area and wearable applications. Advantages such as high transconductance, stability in aqueous electrolytes, cytocompatibility and facile biofunctionalization make them particularly suitable for bioelectronics. Materials with tailored biological properties, for example, modified with enzymes, can be used for OECT-based biosensors. Although OECT-based biosensors have been

tested only *in vitro* so far, *in vivo* applications are envisioned. OECTs can also be fabricated from materials that are optically transparent, allow electromechanical activation[181] and leverage ion transport for drug delivery[182], which makes them suitable as multimodal tools for cell monitoring. Three-dimensional cell culture platforms made of conducting polymers[183] offer the opportunity to control the mechanical, biochemical and electrical microenvironment of a cell and to simultaneously monitor cell behaviour. The combination of high-performance OECT sensors with high-end silicon electronics through heterogeneous integration will facilitate the development of large multiplexed arrays for electrophysiology[184]. By contrast, simple OECT circuits interfaced with sensors for multiplexing, processing and amplification will benefit from the simplicity of an all-organic technology and will be relevant to 'quasi-static' applications such as biosensor arrays. Ion gels, such as those used in organic FETs[185], can render OECTs suitable for printed electronic applications. Moreover, the ability of OECTs to conduct large currents makes them interesting for applications in power electronics. Finally, the first devices for neuromorphic computing using OECTs have already been developed. The next step entails the scaling up of the number of devices and the scaling down of the individual device size to demonstrate the potential of OECT-based neuromorphic computing.

Finally, to discuss OECTs in relation to OFETs, the two devices represent the opposite ends of the same spectrum in terms of operation mechanism. They share many properties and are similar in terms of materials, processes and form factors. However, OECTs are a considerably less mature technology than OFETs. When compared from a gain versus bandwidth perspective (FIG. 5), the transconductance of OECTs is larger than that of OFETs up to a certain frequency, beyond which OFETs have the performance advantage. For a typical microfabricated OECT ($W \times L = 10 \times 10\ \mu m^2$, $d = 100\ nm$), the transconductance is in the range of mS and starts to roll off at kilohertz frequencies. An OFET of similar size with a hole mobility of $1\ cm^2\ V^{-1}\ s^{-1}$ and with $C' = 1\ \mu F\ cm^{-2}$ (dielectric made of a self-assembled monolayer) has a transconductance of around 1 μS, which extends to megahertz frequencies. However, the transconductance of an OECT changes depending on the nature of the electrolyte; for example, a gel or solid electrolyte leads to slower devices. Therefore, the exact frequency at which OECTs lose the performance advantage over OFETs depends on the nature of the electrolyte and therefore on the specific OECT design. Other metrics, such as the ON/OFF ratio, linearity of characteristics, electrical stability and environmental stability, are difficult to compare because they have not been well studied for OECTs. Nevertheless, OECTs have a higher transconductance than OFETs up to a frequency well beyond their roll-off value, suggesting that they can replace OFETs in many applications. However, applications that require the highest possible frequencies, such as in radio frequency identification tags or display driving circuitry, remain difficult areas for the implementation of OECTs. Assuming a similar rate of progress for OECTs as for OFETs, the next few years will bring great progress in OECT technology, which could result in their commercialization.

1. Sze, S. M. & Ng, K. K. *Physics of Semiconductor Devices.* (John Wiley & Sons, 2006).
2. Dimitrakopoulos, C. D. & Malenfant, P. R. L. Organic thin film transistors for large area electronics. *Adv. Mater.* **14**, 99–117 (2002).
3. Venkateshvaran, D. *et al.* Approaching disorder-free transport in high-mobility conjugated polymers. *Nature* **515**, 384–388 (2014).
4. Nikolka, M. *et al.* High operational and environmental stability of high-mobility conjugated polymer field-effect transistors through the use of molecular additives. *Nat. Mater.* **16**, 356–362 (2017).
5. Dodabalapur, A. *et al.* Organic smart pixels. *Appl. Phys. Lett.* **73**, 142–144 (1998).
6. Someya, T. Building bionic skin. *IEEE Spectr.* **50**, 50–56 (2013).
7. Xu, J. *et al.* Highly stretchable polymer semiconductor films through the nanoconfinement effect. *Science* **355**, 59–64 (2017).
8. Torsi, L. *et al.* A sensitivity-enhanced field-effect chiral sensor. *Nat. Mater.* **7**, 412–417 (2008).
9. Knopfmacher, O. *et al.* Highly stable organic polymer field-effect transistor sensor for selective detection in the marine environment. *Nat. Commun.* **5**, 3954 (2014).
10. White, H. S., Kittlesen, G. P. & Wrighton, M. S. Chemical derivatization of an array of 3 gold microelectrodes with polypyrrole — fabrication of a molecule-based transistor. *J. Am. Chem. Soc.* **106**, 5375–5377 (1984).
11. Bernards, D. A. & Malliaras, G. G. Steady-state and transient behavior of organic electrochemical transistors. *Adv. Funct. Mater.* **17**, 3538–3544 (2007).
12. Khodagholy, D. *et al.* High transconductance organic electrochemical transistors. *Nat. Commun.* **4**, 2133 (2013).
13. Elschner, A., Kirchmeyer, S., Lövenich, W., Merker, U. & Reuter, K. in *PEDOT, Principles and Applications of an Intrinsically Conductive Polymer* 113–166 (CRC Press, 2010).
14. Nielsen, C. B. *et al.* Molecular design of semiconducting polymers for high-performance organic electrochemical transistors. *J. Am. Chem. Soc.* **138**, 10252–10259 (2016).
15. Rivnay, J. *et al.* Organic electrochemical transistors with maximum transconductance at zero gate bias. *Adv. Mater.* **25**, 7010–7014 (2013).
16. Khodagholy, D. *et al. In vivo* recordings of brain activity using organic transistors. *Nat. Commun.* **4**, 1575 (2013).
17. Rivnay, J. *et al.* High-performance transistors for bioelectronics through tuning of channel thickness. *Sci. Adv.* **1**, e1400251–e1400251 (2015).
18. Strakosas, X., Bongo, M. & Owens, R. M. The organic electrochemical transistor for biological applications. *J. Appl. Polym. Sci.* **132**, 41735 (2015).
19. Lin, P. & Yan, F. Organic thin-film transistors for chemical and biological sensing. *Adv. Mater.* **24**, 34–51 (2012).
20. Nilsson, D., Robinson, N., Berggren, M. & Forchheimer, R. Electrochemical logic circuits. *Adv. Mater.* **17**, 353–358 (2005).
21. Hütter, P. C., Rothländer, T., Scheipl, G. & Stadlober, B. All screen-printed logic gates based on organic electrochemical transistors. *IEEE Trans. Electron. Devices* **62**, 4231–4236 (2015).
22. Gkoupidenis, P., Schaefer, N., Garlan, B. & Malliaras, G. G. Neuromorphic functions in PEDOT:PSS organic electrochemical transistors. *Adv. Mater.* **27**, 7176–7180 (2015).
23. van de Burgt, Y. *et al.* A non-volatile organic electrochemical device as a low-voltage artificial synapse for neuromorphic computing. *Nat. Mater.* **16**, 414–418 (2017).
24. Proctor, C. M., Rivnay, J. & Malliaras, G. G. Understanding volumetric capacitance in conducting polymers. *J. Polym. Sci. Part B Polym. Phys.* **54**, 1433–1436 (2016).
25. Angione, M. D. *et al.* Interfacial electronic effects in functional biolayers integrated into organic field-effect transistors. *Proc. Natl Acad. Sci. USA* **109**, 6429–6434 (2012).
26. Bowling, R., Packard, R. T. & McCreery, R. L. Mechanism of electrochemical activation of carbon electrodes: role of graphite lattice defects. *Langmuir* **5**, 683–688 (1989).
27. Ranganathan, S. & McCreery, R. L. Electroanalytical performance of carbon films with near-atomic flatness. *Anal. Chem.* **73**, 893–900 (2001).
28. Buzsáki, G. *Rhythms of the Brain.* (Oxford Univ. Press, 2006).
29. Berggren, M., Nilsson, D. & Robinson, N. D. Organic materials for printed electronics. *Nat. Mater.* **6**, 3–5 (2007).
30. Robinson, N. D., Svensson, P.-O., Nilsson, D. & Berggren, M. On the current saturation observed in electrochemical polymer transistors. *J. Electrochem. Soc.* **153**, H39 (2006).
31. Friedlein, J. T., Shaheen, S. E., Malliaras, G. G. & McLeod, R. R. Optical measurements revealing nonuniform hole mobility in organic electrochemical transistors. *Adv. Electron. Mater.* **1**, 1500189 (2015).
32. Kaphle, V., Liu, S., Al-Shadeedi, A., Keum, C.-M. & Lüssem, B. Contact resistance effects in highly doped organic electrochemical transistors. *Adv. Mater.* **28**, 8766–8770 (2016).
33. Friedlein, J. T. *et al.* Influence of disorder on transfer characteristics of organic electrochemical transistors. *Appl. Phys. Lett.* **111**, 023301 (2017).
34. Giovannitti, A. *et al.* N-type organic electrochemical transistors with stability in water. *Nat. Commun.* **7**, 13066 (2016).
35. Laiho, A., Herlogsson, L., Forchheimer, R., Crispin, X. & Berggren, M. Controlling the dimensionality of charge transport in organic thin-film transistors. *Proc. Natl Acad. Sci. USA* **108**, 15069–15073 (2011).

36. Giovannitti, A. *et al.* Controlling the mode of operation of organic transistors through side-chain engineering. *Proc. Natl Acad. Sci. USA* **113**, 12017–12022 (2016).
37. Cicoira, F. *et al.* Influence of device geometry on sensor characteristics of planar organic electrochemical transistors. *Adv. Mater.* **22**, 1012–1016 (2010).
38. Hütter, P. C., Rothländer, T., Haase, A., Trimmel, G. & Stadlober, B. Influence of geometry variations on the response of organic electrochemical transistors. *Appl. Phys. Lett.* **103**, 043308 (2013).
39. Bard, A. J. & Faulkner, L. R. *Electrochemical Methods: Fundamentals and Applications* 2nd edn (Wiley, 2001).
40. Bernards, D. A. *et al.* Enzymatic sensing with organic electrochemical transistors. *J. Mater. Chem.* **18**, 116–120 (2008).
41. Koutsouras, D. A. *et al.* Impedance spectroscopy of spun cast and electrochemically deposited PEDOT:PSS films on microfabricated electrodes with various areas. *ChemElectroChem* **4**, 2321–2327 (2017).
42. Martin, D. C. *et al.* The morphology of poly(3,4-ethylenedioxythiophene). *Polym. Rev.* **50**, 340–384 (2010).
43. Nardes, A. M. *et al.* Microscopic understanding of the anisotropic conductivity of PEDOT: PSS thin films. *Adv. Mater.* **19**, 1196–1200 (2007).
44. Wang, Y. *et al.* A highly stretchable, transparent, and conductive polymer. *Sci. Adv.* **3**, e1602076 (2017).
45. Stavrinidou, E. *et al.* Direct measurement of ion mobility in a conducting polymer. *Adv. Mater.* **25**, 4488–4493 (2013).
46. Rivnay, J. *et al.* Structural control of mixed ionic and electronic transport in conducting polymers. *Nat. Commun.* **7**, 11287 (2016).
47. Inal, S., Malliaras, G. G. & Rivnay, J. Optical study of electrochromic moving fronts for the investigation of ion transport in conducting polymers. *J. Mater. Chem. C* **4**, 3942–3947 (2016).
48. Asplund, M., Nyberg, T. & Inganas, O. Electroactive polymers for neural interfaces. *Polym. Chem.* **1**, 1374–1391 (2010).
49. ElMahmoudy, M. *et al.* Tailoring the electrochemical and mechanical properties of PEDOT:PSS films for bioelectronics. *Macromol. Mater. Eng.* **17**, 1600497 (2017).
50. Håkansson, A. *et al.* Effect of (3-glycidyloxypropyl) trimethoxysilane (GOPS) on the electrical properties of PEDOT:PSS films. *J. Polym. Sci. Part B Polym. Phys.* **55**, 814–820 (2017).
51. Mantione, D. *et al.* Low-temperature cross-linking of PEDOT:PSS films using divinylsulfone. *ACS Appl. Mater. Interfaces* **9**, 18254–18262 (2017).
52. Olivier, Y. *et al.* 25th anniversary article: high-mobility hole and electron transport conjugated polymers: how structure defines function. *Adv. Mater.* **26**, 2119–2136 (2014).
53. Kim, D.-H. *et al.* in *Indwelling Neural Implants: Strategies for Contending with the In-Vivo Environment* (ed. Reichert, W. M.) 165–207 (CRC Press/Taylor & Francis, 2008).
54. Berggren, M. & Richter-Dahlfors, A. Organic bioelectronics. *Adv. Mater.* **19**, 3201–3213 (2007).
55. Inal, S. *et al.* Organic electrochemical transistors based on PEDOT with different anionic polyelectrolyte dopants. *J. Polym. Sci. Part B Polym. Phys.* **54**, 147–151 (2016).
56. Inal, S. *et al.* A high transconductance accumulation mode electrochemical transistor. *Adv. Mater.* **26**, 7450–7455 (2014).
57. Zeglio, E. *et al.* Conjugated polyelectrolyte blends for electrochromic and electrochemical transistor devices. *Chem. Mater.* **27**, 6385–6393 (2015).
58. Strakosas, X. *et al.* A facile biofunctionalisation route for solution processable conducting polymer devices. *J. Mater. Chem. B* **2**, 2537 (2014).
59. Skotheim, T. A. & Reynolds, J. R. *Handbook of Conducting Polymers. Conjugated Polymers: Processing and Applications.* (CRC Press, 2007).
60. Winther-Jensen, B. & West, K. Vapor-phase polymerization of 3,4-ethylenedioxythiophene: a route to highly conducting polymer surface layers. *Macromolecules* **37**, 4538–4543 (2004).
61. Jimison, L. H. *et al.* PEDOT:TOS with PEG: a biofunctional surface with improved electronic characteristics. *J. Mater. Chem.* **22**, 19498–19505 (2012).
62. Bongo, M. *et al.* PEDOT:gelatin composites mediate brain endothelial cell adhesion. *J. Mater. Chem. B* **1**, 3860–3867 (2013).
63. Winther-Jensen, B., Kolodziejczyk, B. & Winther-Jensen, O. New one-pot poly(3,4-ethylenedioxythiophene): poly(tetrahydrofuran) memory material for facile fabrication of memory organic electrochemical transistors. *APL Mater.* **3**, 014903 (2015).
64. Khodagholy, D. *et al.* Organic electrochemical transistor incorporating an ionogel as a solid state electrolyte for lactate sensing. *J. Mater. Chem.* **22**, 4440–4443 (2012).
65. Nilsson, D., Kugler, T., Svensson, P. O. & Berggren, M. An all-organic sensor-transistor based on a novel electrochemical transducer concept printed electrochemical sensors on paper. *Sens. Actuators B Chem.* **86**, 193–197 (2002).
66. Tarabella, G. *et al.* Effect of the gate electrode on the response of organic electrochemical transistors. *Appl. Phys. Lett.* **97**, 123304 (2010).
67. Tang, H., Lin, P., Chan, H. L. W. & Yan, F. Highly sensitive dopamine biosensors based on organic electrochemical transistors. *Biosens. Bioelectron.* **26**, 4559–4563 (2011).
68. Tang, H. *et al.* Conducting polymer transistors making use of activated carbon gate electrodes. *ACS Appl. Mater. Interfaces* **7**, 969–973 (2015).
69. Diaz, A. F. & Castillo, J. I. A polymer electrode with variable conductivity: polypyrrole. *J. Chem. Soc., Chem. Commun.* 397–398 (1980).
70. Thackeray, J. W., White, H. S. & Wrighton, M. S. Poly(3-methylthiophene)-coated electrodes: optical and electrical properties as a function of redox potential and amplification of electrical and chemical signals using poly(3-methylthiophene)-based microelectrochemical transistors. *J. Phys. Chem.* **89**, 5133–5140 (1985).
71. Paul, E. W., Ricco, A. J. & Wrighton, M. S. Resistance of polyaniline films as a function of electrochemical potential and the fabrication of polyaniline-based microelectronic devices. *J. Phys. Chem.* **89**, 1441–1447 (1985).
72. Kittlesen, G. P., White, H. S. & Wrighton, M. S. Chemical derivatization of microelectrode arrays by oxidation of pyrrole and n-methylpyrrole — fabrication of molecule-based electronic devices. *J. Am. Chem. Soc.* **106**, 7389–7396 (1984).
73. Jernigan, J. C., Wilbourn, K. O. & Murray, R. W. A benzimidazobenzophenanthroline polymer molecular transistor fabricated using club sandwich electrodes. *J. Electroanal. Chem.* **222**, 193–200 (1987).
74. Takashima, W., Sasano, K., Asano, T. & Kaneto, K. Electroplasticity memory devices using conducting polymers and solid polymer electrolytes. *Polym. Int.* **27**, 249–253 (1992).
75. Kaneto, K., Asano, T. & Takashima, W. Memory device using a conducting polymer and solid polymer electrolyte. *Jpn J. Appl. Phys.* **30**, L215 (1991).
76. Matsue, T., Nishizawa, M., Sawaguchi, T. & Uchida, I. An enzyme switch sensitive to NADH. *J. Chem. Soc., Chem. Commun.* 1029–1031 (1991).
77. Saxena, V., Shirodkar, V. & Prakash, R. A comparative study of a polyindole-based microelectrochemical transistor in aqueous and non-aqueous electrolytes. *J. Solid State Electrochem.* **4**, 231–233 (2000).
78. Bartlett, P. N. & Birkin, P. R. A. Microelectrochemical enzyme transistor responsive to glucose. *Anal. Chem.* **66**, 1552–1559 (1994).
79. Bartlett, P. N. Measurement of low glucose concentrations using a microelectrochemical enzyme transistor. *Analyst* **123**, 387–392 (1998).
80. Bartlett, P. N., Birkin, P. R., Wang, J. H., Palmisano, F. & De Benedetto, G. An enzyme switch employing direct electrochemical communication between horseradish peroxidase and a poly(aniline) film. *Anal. Chem.* **70**, 3685–3694 (1998).
81. Rani, V. & Santhanam, K. S. V. Polycarbazole-based electrochemical transistor. *J. Solid State Electrochem.* **2**, 99–101 (1998).
82. Heywang, G. & Jonas, F. Poly(alkylenedioxythiophene) s — new, very stable conducting polymers. *Adv. Mater.* **4**, 116–118 (1992).
83. Qibing, P., Zuccarello, G., Ahlskog, M. & Inganäs, O. Electrochromic and highly stable poly(3,4-ethylenedioxythiophene) switches between opaque blue-black and transparent sky blue. *Polymer* **35**, 1347–1351 (1994).
84. Groenendaal, L., Jonas, F., Freitag, D., Pielartzik, H. & Reynolds, J. R. Poly(3,4-ethylenedioxythiophene) and its derivatives: past, present, and future. *Adv. Mater.* **12**, 481–494 (2000).
85. Morvant, Mark, C. & Reynolds, John, R. In situ conductivity studies of poly(3,4-ethylenedioxythiophene). *Synth. Met.* **92**, 57–61 (1998).
86. Carlberg, J. C. & Inganäs, O. Fast optical spectroscopy of the electrochemical doping of poly(3,4-ethylenedioxythiophene). *J. Electrochem. Soc.* **145**, 3810–3814 (1998).
87. Nilsson, D. *et al.* Bi-stable and dynamic current modulation in electrochemical organic transistors. *Adv. Mater.* **14**, 51–54 (2002).
88. Epstein, A. J., Hsu, F.-C., Chiou, N.-R. & Prigodin, V. N. Electric-field induced ion-leveraged metal–insulator transition in conducting polymer-based field effect devices. *Curr. Appl. Phys.* **2**, 339–343 (2002).
89. Andersson, P. *et al.* Active matrix displays based on all-organic electrochemical smart pixels printed on paper. *Adv. Mater.* **14**, 1460–1464 (2002).
90. Mabeck, J. T. *et al.* Microfluidic gating of an organic electrochemical transistor. *Appl. Phys. Lett.* **87**, 013503 (2005).
91. Bernards, D. A., Malliaras, G. G., Toombes, G. E. S. & Gruner, S. M. Gating of an organic transistor through a bilayer lipid membrane with ion channels. *Appl. Phys. Lett.* **89**, 053505 (2006).
92. Curto, V. F. An organic transistor platform with integrated microfluidics for in-line multi-parametric *in vitro* cell monitoring. *Microsystems Nanoengineer.* **3**, 17028 (2017).
93. Alam, M. M., Wang, J., Guo, Y., Lee, S. P. & Tseng, H.-R. Electrolyte-gated transistors based on conducting polymer nanowire junction arrays. *J. Phys. Chem. B* **109**, 12777–12784 (2005).
94. Wan, A. M.-D. *et al.* 3D conducting polymer platforms for electrical control of protein conformation and cellular functions. *J. Mater. Chem. B* **3**, 5040–5048 (2015).
95. Tehrani, P. *et al.* Patterning polythiophene films using electrochemical over-oxidation. *Smart Mater. Struct.* **14**, N21–N25 (2005).
96. Mannerbro, R., Ranlöf, M., Robinson, N. & Forchheimer, R. Inkjet printed electrochemical organic electronics. *Synth. Met.* **158**, 556–560 (2008).
97. Kolodziejczyk, B., Winther-Jensen, O., Pereira, B. A., Nair, S. S. & Winther-Jensen, B. Patterning of conducting layers on breathable substrates using laser engraving for gas sensors. *J. Appl. Polym. Sci.* **132**, 42356 (2015).
98. Gualandi, I. *et al.* Textile organic electrochemical transistors as a platform for wearable biosensors. *Sci. Rep.* **6**, 33637 (2016).
99. Hamedi, M., Forchheimer, R. & Inganas, O. Towards woven logic from organic electronic fibres. *Nat. Mater.* **6**, 357–362 (2007).
100. Wang, Y. *et al.* Ion sensors based on novel fiber organic electrochemical transistors for lead ion detection. *Anal. Bioanal. Chem.* **408**, 5779–5787 (2016).
101. Tarabella, G. *et al.* A single cotton fiber organic electrochemical transistor for liquid electrolyte saline sensing. *J. Mater. Chem.* **22**, 23830–23834 (2012).
102. Kawahara, J. *et al.* Reconfigurable sticker label electronics manufactured from nanofibrillated cellulose-based self-adhesive organic electronic materials. *Org. Electron.* **14**, 3061–3069 (2013).
103. Malti, A. *et al.* An organic mixed ion–electron conductor for power electronics. *Adv. Sci.* **3**, 1500305 (2016).
104. Stavrinidou, E. *et al.* Electronic plants. *Sci. Adv.* **1**, e1501136 (2015).
105. Rivnay, J., Owens, R. M. & Malliaras, G. G. The rise of organic bioelectronics. *Chem. Mater.* **26**, 679–685 (2014).
106. Someya, T., Bao, Z. & Malliaras, G. G. The rise of plastic bioelectronics. *Nature* **540**, 379–385 (2016).
107. Williamson, A. *et al.* Localized neuron stimulation with organic electrochemical transistors on delaminating depth probes. *Adv. Mater.* **27**, 4405–4410 (2015).
108. Lee, W. *et al.* Integration of organic electrochemical and field-effect transistors for ultraflexible, high temporal resolution electrophysiology arrays. *Adv. Mater.* **28**, 9722–9728 (2016).
109. Campana, A., Cramer, T., Simon, D. T., Berggren, M. & Biscarini, F. Electrocardiographic recording with conformable organic electrochemical transistor fabricated on resorbable bioscaffold. *Adv. Mater.* **26**, 3874–3878 (2014).

110. Leleux, P. *et al.* Organic electrochemical transistors for clinical applications. *Adv. Healthc. Mater.* **4**, 142 (2014).
111. Braendlein, M., Lonjaret, T., Leleux, P., Badier, J.-M. & Malliaras, G. G. Voltage amplifier based on organic electrochemical transistor. *Adv. Sci.* **4**, 1600247 (2017).
112. Uguz, I. *et al.* Autoclave sterilization of PEDOT:PSS electrophysiology devices. *Adv. Healthc. Mater.* **5**, 3094–3098 (2016).
113. Yao, C., Li, Q., Guo, J., Yan, F. & Hsing, I. M. Rigid and flexible organic electrochemical transistor arrays for monitoring action potentials from electrogenic cells. *Adv. Healthc. Mater.* **4**, 528–533 (2014).
114. Gu, X., Yao, C., Liu, Y. & Hsing, I.-M. 16-channel organic electrochemical transistor array for in vitro conduction mapping of cardiac action potential. *Adv. Healthc. Mater.* **5**, 2345–2351 (2016).
115. Lin, P., Yan, F., Yu, J. J., Chan, H. L. W. & Yang, M. The application of organic electrochemical transistors in cell-based biosensors. *Adv. Mater.* **22**, 3655–3660 (2010).
116. Jimison, L. H. *et al.* Measurement of barrier tissue integrity with an organic electrochemical transistor. *Adv. Mater.* **24**, 5919–5923 (2012).
117. Yao, C. *et al.* Organic electrochemical transistor array for recording transepithelial ion transport of human airway epithelial cells. *Adv. Mater.* **25**, 6575–6580 (2013).
118. Romeo, A. *et al.* Drug-induced cellular death dynamics monitored by a highly sensitive organic electrochemical system. *Biosens. Bioelectron.* **68**, 791–797 (2015).
119. Ramuz, M., Hama, A., Rivnay, J., Leleux, P. & Owens, R. M. Monitoring of cell layer coverage and differentiation with the organic electrochemical transistor. *J. Mater. Chem. B* **3**, 5971–5977 (2015).
120. Huerta, M., Rivnay, J., Ramuz, M., Hama, A. & Owens, R. M. Early detection of nephrotoxicity in vitro using a transparent conducting polymer device. *Appl. Vitro Toxicol.* **2**, 17–25 (2016).
121. Faria, G. C. *et al.* Organic electrochemical transistors as impedance biosensors. *MRS Commun.* **4**, 189–194 (2014).
122. Zhang, Y. *et al.* Supported lipid bilayer assembly on PEDOT:PSS films and transistors. *Adv. Funct. Mater.* **26**, 7304–7313 (2016).
123. Rivnay, J. *et al.* Organic electrochemical transistors for cell-based impedance sensing. *Appl. Phys. Lett.* **106**, 043301 (2015).
124. Rivnay, J. *et al.* Using white noise to gate organic transistors for dynamic monitoring of cultured cell layers. *Sci. Rep.* **5**, 11613 (2015).
125. Ramuz, M. *et al.* Combined optical and electronic sensing of epithelial cells using planar organic transistors. *Adv. Mater.* **26**, 7083–7090 (2014).
126. Tria, S. A. *et al.* Dynamic monitoring of *Salmonella* typhimurium infection of polarized epithelia using organic transistors. *Adv. Healthc. Mater.* **3**, 1053–1060 (2014).
127. Huerta, M., Rivnay, J., Ramuz, M., Hama, A. & Owens, R. M. Research update: electrical monitoring of cysts using organic electrochemical transistors. *APL Mater.* **3**, 030701 (2015).
128. Bolin, M. H. *et al.* Active control of epithelial cell-density gradients grown along the channel of an organic electrochemical transistor. *Adv. Mater.* **21**, 4379–4382 (2009).
129. Lin, P., Yan, F. & Chan, H. L. W. Ion-sensitive properties of organic electrochemical transistors. *ACS Appl. Mater. Interfaces* **2**, 1637–1641 (2010).
130. Sessolo, M., Rivnay, J., Bandiello, E., Malliaras, G. G. & Bolink, H. J. Ion-selective organic electrochemical transistors. *Adv. Mater.* **26**, 4803–4807 (2014).
131. Zhu, Z. T. *et al.* A simple poly(3,4-ethylene dioxythiophene)/poly(styrene sulfonic acid) transistor for glucose sensing at neutral pH. *Chem. Commun.* 1556–1557 (2004).
132. Tang, H., Yan, F., Lin, P., Xu, J. & Chan, H. L. W. Highly sensitive glucose biosensors based on organic electrochemical transistors using platinum gate electrodes modified with enzyme and nanomaterials. *Adv. Funct. Mater.* **21**, 2264–2272 (2011).
133. Liao, C., Zhang, M., Niu, L., Zheng, Z. & Yan, F. Highly selective and sensitive glucose sensors based on organic electrochemical transistors with graphene-modified gate electrodes. *J. Mater. Chem. B* **1**, 3820–3829 (2013).
134. Yang, S. Y. *et al.* Integration of a surface-directed microfluidic system with an organic electrochemical transistor array for multi-analyte biosensors. *Lab Chip* **9**, 704–708 (2009).
135. Pappa, A.-M. *et al.* Organic transistor arrays integrated with finger-powered microfluidics for multianalyte saliva testing. *Adv. Healthc. Mater.* **5**, 2295–2302 (2016).
136. Battista, E. *et al.* Enzymatic sensing with laccase-functionalized textile organic biosensors. *Org. Electron.* **40**, 51–57 (2017).
137. Bihar, E. *et al.* A disposable paper breathalyzer with an alcohol sensing organic electrochemical transistor. *Sci. Rep.* **6**, 27582 (2016).
138. Scheiblin, G., Coppard, R., Owens, R. M., Mailley, P. & Malliaras, G. G. Referenceless pH sensor using organic electrochemical transistors. *Adv. Mater. Technol.* **2**, 1600141 (2017).
139. Liao, C., Mak, C., Zhang, M., Chan, H. L. W. & Yan, F. Flexible organic electrochemical transistors for highly selective enzyme biosensors and used for saliva testing. *Adv. Mater.* **27**, 676–681 (2015).
140. Braendlein, M. *et al.* Lactate detection in tumor cell cultures using organic transistor circuits. *Adv. Mater.* **29**, 1605744 (2017).
141. Tybrandt, K., Kollipara, S. B. & Berggren, M. Organic electrochemical transistors for signal amplification in fast scan cyclic voltammetry. *Sens. Actuators B Chem.* **195**, 651–656 (2014).
142. Gualandi, I. *et al.* Selective detection of dopamine with an all PEDOT:PSS organic electrochemical transistor. *Sci. Rep.* **6**, 35419 (2016).
143. Mak, C. H. *et al.* Highly-sensitive epinephrine sensors based on organic electrochemical transistors with carbon nanomaterial modified gate electrodes. *J. Mater. Chem. C* **3**, 6532–6538 (2015).
144. Lin, P., Luo, X., Hsing, I. M. & Yan, F. Organic electrochemical transistors integrated in flexible microfluidic systems and used for label-free DNA sensing. *Adv. Mater.* **23**, 4035–4040 (2011).
145. He, R.-X. *et al.* Detection of bacteria with organic electrochemical transistors. *J. Mater. Chem.* **22**, 22072–22076 (2012).
146. Berggren, M. *et al.* Browsing the real world using organic electronics, Si-chips, and a human touch. *Adv. Mater.* **28**, 1911–1916 (2016).
147. Andersson, P., Forchheimer, R., Tehrani, P. & Berggren, M. Printable all-organic electrochromic active-matrix displays. *Adv. Funct. Mater.* **17**, 3074–3082 (2007).
148. Tao, X., Koncar, V. & Dufour, C. Geometry pattern for the wire organic electrochemical textile transistor. *J. Electrochem. Soc.* **158**, H572–H577 (2011).
149. Zirkl, M. *et al.* An all-printed ferroelectric active matrix sensor network based on only five functional materials forming a touchless control interface. *Adv. Mater.* **23**, 2069–2074 (2011).
150. Keshmiri, Forchheimer & Tu. in *7th International Conference on Computer Aided Design for Thin-Film Transistor Technologies (CAD-TFT)* http://dx.doi.org/10.1109/CAD-TFT.2016.7785048 (Beijing, 2016).
151. Rothlander, T. *et al.* Nanoimprint lithography-structured organic electrochemical transistors and logic circuits. *IEEE Trans. Electron. Devices* **61**, 1515–1519 (2014).
152. Brooke, R. *et al.* Inkjet printing and vapor phase polymerization: patterned conductive PEDOT for electronic applications. *J. Mater. Chem. C* **1**, 3353–3358 (2013).
153. Svensson, P. O., Nilsson, D., Forchheimer, R. & Berggren, M. A sensor circuit using reference-based conductance switching in organic electrochemical transistors. *Appl. Phys. Lett.* **93**, 203301 (2008).
154. Strukov, D. B., Snider, G. S., Stewart, D. R. & Williams, R. S. The missing memristor found. *Nature* **453**, 80–83 (2008).
155. Merolla, P. A. *et al.* A million spiking-neuron integrated circuit with a scalable communication network and interface. *Science* **345**, 668–673 (2014).
156. Prezioso, M. *et al.* Training and operation of an integrated neuromorphic network based on metal-oxide memristors. *Nature* **521**, 61–64 (2015).
157. Erokhin, V., Berzina, T. & Fontana, M. P. Hybrid electronic device based on polyaniline-polyethyleneoxide junction. *J. Appl. Phys.* **97**, 064501 (2005).
158. Berzina, T. *et al.* Optimization of an organic memristor as an adaptive memory element. *J. Appl. Phys.* **105**, 124515 (2009).
159. Emelyanov, A. V. *et al.* First steps towards the realization of a double layer perceptron based on organic memristive devices. *AIP Adv.* **6**, 111301 (2016).
160. Cifarelli, A., Berzina, T., Parisini, A., Erokhin, V. & Iannotta, S. Polysaccarides-based gels and solid-state electronic devices with memresistive properties: synergy between polyaniline electrochemistry and biology. *AIP Adv.* **6**, 111302 (2016).
161. Das, B. C., Pillai, R. G., Wu, Y. & McCreery, R. L. Redox-gated three-terminal organic memory devices: effect of composition and environment on performance. *ACS Appl. Mater. Interfaces* **5**, 11052–11058 (2013).
162. Das, B. C., Szeto, B., James, D. D., Wu, Y. & McCreery, R. L. Ion transport and switching speed in redox-gated 3-terminal organic memory devices. *J. Electrochem. Soc.* **161**, H831–H838 (2014).
163. Xu, W., Min, S.-Y., Hwang, H. & Lee, T.-W. Organic core-sheath nanowire artificial synapses with femtojoule energy consumption. *Sci. Adv.* **2**, e1501326 (2016).
164. Gkoupidenis, P., Schaefer, N., Strakosas, X., Fairfield, J. A. & Malliaras, G. G. Synaptic plasticity functions in an organic electrochemical transistor. *Appl. Phys. Lett.* **107**, 263302 (2015).
165. Gkoupidenis, P., Koutsouras, D. A., Lonjaret, T., Fairfield, J. A. & Malliaras, G. G. Orientation selectivity in a multi-gated organic electrochemical transistor. *Sci. Rep.* **6**, 27007 (2016).
166. Gkoupidenis, P., Koutsouras, D. A. & Malliaras, G. G. Neuromorphic device architectures with global connectivity through electrolyte gating. *Nat. Commun.* **8**, 15448 (2017).
167. Xuan, Y., Sandberg, M., Berggren, M. & Crispin, X. An all-polymer-air PEDOT battery. *Org. Electron.* **13**, 632–637 (2012).
168. Fuller, E. J. *et al.* Li-ion synaptic transistor for low power analog computing. *Adv. Mater.* **29**, 1604310 (2017).
169. Fabiano, S. *et al.* Ferroelectric polarization induces electronic nonlinearity in ion-doped conducting polymers. *Sci. Adv.* **3**, e1700345 (2017).
170. Shen, Y. L., Hosseini, A. R., Wong, M. H. & Malliaras, G. G. How to make ohmic contacts to organic semiconductors. *ChemPhysChem* **5**, 16–25 (2004).
171. Koch, N. Organic electronic devices and their functional interfaces. *ChemPhysChem* **8**, 1438–1455 (2007).
172. Giridharagopal, R. *et al.* Electrochemical strain microscopy probes morphology-induced variations in ion uptake and performance in organic electrochemical transistors. *Nat. Mater.* **16**, 737–742 (2017).
173. Borsenberger, P. M. & Weiss, D. S. *Organic Photoreceptors for Xerography* (Marcel Dekker, 1998).
174. Sirringhaus, H. 25th anniversary article: organic field-effect transistors: the path beyond amorphous silicon. *Adv. Mater.* **26**, 1319–1335 (2014).
175. Friedlein, J. T., Donahue, M. J., Shaheen, S. E., Malliaras, G. G. & McLeod, R. R. Microsecond response in organic electrochemical transistors: exceeding the ionic speed limit. *Adv. Mater.* **28**, 8398–8404 (2016).
176. Sideris, P., Siskos, S. & Malliaras, G. in *6th International Conference on Modern Circuits and Systems Technologies (MOCAST)* http://dx.doi.org/10.1109/MOCAST.2017.7937645 (Thessaloniki, 2016).
177. Inal, S., Malliaras, G. G. & Rivnay, J. Benchmarking organic mixed conductors for transistors. *Nat. Commun.* **8**, 1767 (2017).
178. Stavrinidou, E. *et al.* Engineering hydrophilic conducting composites with enhanced ion mobility. *Phys. Chem. Chem. Phys.* **16**, 2275–2279 (2014).
179. Zeglio, E., Eriksson, J., Gabrielsson, R., Solin, N. & Inganäs, O. Highly stable conjugated polyelectrolytes for water-based hybrid mode electrochemical transistors. *Adv. Mater.* **29**, 1605787 (2017).
180. Pacheco-Moreno, C. M. *et al.* The importance of materials design to make ions flow: toward novel materials platforms for bioelectronics applications. *Adv. Mater.* **29**, 1604446 (2017).
181. Smela, E. Conjugated polymer actuators. *MRS Bull.* **33**, 197–204 (2008).
182. Isaksson, J. *et al.* Electronic control of Ca^{2+} signalling in neuronal cells using an organic electronic ion pump. *Nat. Mater.* **6**, 673–679 (2007).
183. Inal, S. *et al.* Conducting polymer scaffolds for hosting and monitoring 3D cell culture. *Adv. Biosyst.* **1**, 1700052 (2017).

184. Viventi, J. *et al.* Flexible, foldable, actively multiplexed, high-density electrode array for mapping brain activity *in vivo*. *Nat. Neurosci.* **14**, 1599–1605 (2011).
185. Cho, J. H. *et al.* Printable ion-gel gate dielectrics for low-voltage polymer thin-film transistors on plastic. *Nat. Mater.* **7**, 900–906 (2008).

Acknowledgements
The authors gratefully acknowledge financial support from the National Science Foundation, DMR award 1507826 (A.S.); ERC CoG IMBIBE, action number 723951 (R.M.O.); the STIAS, Knut and Alice Wallenberg Foundation, SSF and Önnesjöstiftelsen (M.B.); the European Union's Horizon 2020 Research and Innovation Programme under grant agreement No. 732032 (BrainCom) (G.G.M.) and King Abdullah University of Science and Technology (KAUST) Office of Sponsored Research (OSR) under award No. OSR-2016-CRG5-3003 (S.I., G.G.M.).

Author contributions
All authors contributed equally to the preparation of this manuscript.

Competing interest statement
The authors declare no competing interests.

How to cite this article
Rivnay, J., Inal, S., Salleo, A., Owens, R.M., Berggren, M., Malliaras, G.G. Organic electrochemical transistors. *Nat. Rev. Mater.* **3**, 17086 (2018).

FURTHER INFORMATION
Clevios Conductive Polymers: https://www.heraeus.com/en/group/products_and_solutions_group/conductive_polymers/conductive-polymers-home.aspx
Agfa Specialty Products – Orgacon™ Electronic Materials: http://www.agfa.com/specialty-products/solutions/conductive-materials/

ALL LINKS ARE ACTIVE IN THE PDF